Electromagnetic impedance system for mapping the shallow subsurface

Hung-Wen Tseng[1)], Ki Ha Lee[1)], and Alex Becker[2)]
1) Earth Sciences Div., Lawrence Berkeley National Laboratory, Berkeley, California, USA
2) Dept. of Civil and Environmental Engineering, University of California, Berkeley, USA

Abstract: Non-invasive, high-resolution imaging of shallow subsurface is one of the key elements for successfully delineating buried waste, detecting unexploded ordinance, verifying and monitoring of containment structures, and other environmental applications. Electromagnetic (EM) measurements at frequencies between 1 and 100 MHz are important for such applications, because the induction number of many targets is small and the ability to determine the dielectric permittivity in addition to electrical conductivity of the subsurface is possible. Earlier workers were successful in developing systems for detecting anomalous areas, but no quantifiable information was accurately determined. For high-resolution imaging, accurate measurements are necessary so the field data can be mapped into the space of subsurface parameters. We have been developing a non-invasive method for accurately mapping the electrical conductivity and dielectric permittivity of the shallow subsurface using the EM impedance approach. Electric and magnetic sensors are being tested to ensure that the quality of the data collected with the high-frequency impedance (HFI) system is enough to support high-resolution, multi-dimensional imaging techniques. Additional efforts are being made in modifying and further developing existing sensors and transmitters for improved imaging capability and data acquisition efficiency.

1. Introduction

Accurate information of electrical conductivity and permittivity (water content) are useful in near-surface engineering, and increasingly more important in environmental studies. Traditionally, DC resistivity and loop-loop induction measurements with small spacings have served adequately to determine very near-surface resistivity since the effect of electrical conduction dominates in this low frequency band. However, the DC resistivity and induction methods suffer from lack of resolution and their insensitivity to moisture content. At high frequencies dielectric property dominates, and for this reason the ground-penetrating radar (GPR) has been widely used to investigate shallow subsurface moisture content. While GPR can provide excellent resolution, the method is often limited in its depth of investigation and produces qualitative images with little information concerning subsurface intrinsic electrical properties. The limitation in penetration depth is due to the strong attenuation of high-frequency EM waves in conductive media. DC resistivity methods tend to be slow and expensive in application. Furthermore, the general requirement of planting electrodes in the earth can be undesirably invasive in hazardous environments. Low-frequency inductive EM techniques are almost as rapid as GPR but are frequently less informative, particularly in complex environments.

Using the frequency band between 100 kHz and 100 MHz, which bridges the spectral gap between traditional EM induction methods and GPR, we have been developing a high-frequency impedance (HFI) system (Lee and Becker, 2001). The HFI system offers the capability of determining both resistivity and permittivity at depths to a few meters. Being surface-based and completely non-invasive, it is also a rapid and inexpensive technique for acquiring field data. Song *et al.* (2002) provide an analysis of a plane-wave HFI technique to operate in this spectral

region. As a practical matter, generating plane waves at these frequencies is inconvenient because of the difficulty involved in building a powerful enough transmitter for increased propagation distance, and the interference its signal will encounter with other EM device users. Frangos (2001) completed a proof-of-concept form of the HFI system utilizing off-the-shelf instrumentation, and it has been tested in controlled field conditions. The incident EM wave was generated by a magnetic loop and far- and near-field EM wave can both be utilized with the source. The system determines the EM impedance at selected frequencies between 100 kHz and 30 MHz from direct measurement of continuous wave electric and magnetic fields at source-to-detector separations between four and sixteen meters. Encouraged with the success of the prototype, we have been upgrading the system to improve its reliability and accuracy, and to extend the operating frequency to 100 MHz.

2. Theoretical background and field measurements

The electrical conductivity and dielectric permittivity determine the behavior of EM fields as they diffuse and travel through subsurface materials. The EM fields may be measured on or above the ground surface. For practical considerations, impedance, the ratio of the electric field to the corresponding orthogonal magnetic field, is used to infer the subsurface electrical properties.

For plane wave incidence, the surface impedance, *Z*, on top of a homogeneous isotropic medium for a fixed angular frequency, w, can be derived as

$$Z = \frac{E_x}{H_y} = \frac{\mu\omega}{\sqrt{\varepsilon\mu\omega^2 - i\mu\sigma\omega}} \quad ,$$

where *Ex* and *Hy* are orthogonal electric and magnetic fields; ε is the dielectric permittivity; μ is the magnetic permeability; σ is the electric conductivity; and $i = \sqrt{-1}$ is the imaginary operator. The plane-wave impedance, as is shown, is useful in understanding the relationship between the impedance and electrical parameters. Apparently, the impedance is most affected by the dielectric permittivity at high frequencies and by the electrical conductivity at low frequencies. In practice, however, it is preferable to utilize the general EM impedance, $Z = E_x / H_y$, where fields are not plane wave anymore. This is because power and signal strength considerations require relatively close separations between the transmitter and receiver. The general form of impedance over a layered earth can be easily calculated using the modeling program, EM1D.

To demonstrate the relationship between the general EM impedance and the electrical properties, a three-layer model as sketched in Figure 1(a) is considered. The model represents the near-surface electrical structure of a vineyard in northern California selected for monitoring water content in the soil. Due to soil types and various water content, the soil resistivity are set to 40, 10 and 40 ohm-m and the dielectric constants 16, 19, and 25 from the top to the bottom layers. The thickness of the top and the second layers are 0.5 and 1 m, respectively. Using a magnetic loop dipole source placed 1 m above the ground surface and polarized in the horizontal *y*-direction, we calculated the electric field in the horizontal *x*-direction, E_x, and the magnetic field in the *y*-direction, H_y, at the same height and 8 m from the source. From these fields we obtained the EM impedance by taking the ratio, i.e. E_x / H_y. This setup is similar to the coplanar loop-loop EM method, but electric field is also required at the observation location for the impedance estimation. The amplitude and phase of the impedance for this model over the frequency range from 100 kHz and 100 MHz are represented by the bold solid line in Figure 1(b)

and 1(c), respectively. A perturbation of the dielectric constant of the top layer from 16 to 13 results in a different impedance as represented by the solid circles in the figure, while a change in resistivity of the top layer from 40 to 80 ohm-m (open circles) also reveals the sensitivity of the impedance to subsurface electrical properties. While keeping both parameters in each layer intact but increasing the thickness of the top layer by 0.1 m to 0.6 m, the impedance expressed in crosses in Figure 1(b) and 1(c) also shows pronounced change at almost all frequencies, especially in the amplitude.

3. Instrumentation

Quantitative measurement of broadband high-frequency EM fields near the earth's surface is a difficult task. Radio engineers have directed their efforts toward minimizing the influence of the earth on system behavior. In applied geophysics, just the opposite is desired. The HFI system described in Frangos (2001) is primarily composed of a transmitting source (a loop transmitter with a diameter of 46 cm) emitting continuous sinusoidal EM fields at selected frequencies from 100 kHz to 30 MHz. A stub dipole and a loop antenna have been used to detect the electric and magnetic fields, respectively. A portable computer is used for automatically changing the source frequency and recording the readings from the electrical and the magnetic antennae. All the four units are interconnected via optical links. Pictures of the three antennae are displayed in Figure 2.

The system looks simple at first glance, however, accurate measurement of the absolute electric and magnetic field at this frequency range is difficult, especially for the electric field. Our experience indicates that the electric field is often contaminated with stray pick-ups caused by the wiring attached to the antenna. We have been able to identify the main part of the pick-ups by making measurements twice in reversed polarizations. The estimated pick-up is used to make a correction of each measurement. The correction is valuable in improving data quality of the existing system, but it requires repeat measurements in reversed polarizations, thereby requiring additional acquisition time. Furthermore, the correction appears to be only effective in eliminating the first-order pick-up by wires. The other spurious noise caused by the interferences of protruding electronics components near the center and at the base of the receiver unit remains unchecked. To make a fundamental improvement to the existing sensor, we started redesigning the sensor by miniaturizing the electronics components and replacing all wires with optical fibers. The redesigned and repackaged stub antenna is displayed in Figure 3. All electronic components, including power supply and amplifiers, have been miniaturized and packaged together and positioned at the center of the stub antenna. All communication is done via optical fibers directly attached to the central electronics box. Figure 4 illustrates improvement in electric field measurements using the redesigned stub antenna over the old one. Figure 4(a) shows the comparison of the electric field (dots) with the old antenna in one direction and the electric field (line) with the antenna in the reversed direction. These two measurements are significantly different, especially at the high frequency end. However, the pick-up by the wires can be estimated by summing two measurements of opposite polarizations and is subtracted from corresponding observations to obtain the correct readings. The result is shown in Figure 4(b). The corrected data compare reasonably well except for those at frequencies below 0.3 MHz and around 10 MHz. Finally, the redesigned stub antenna (Figure 3) was used to measure electric fields. Figure 4(c) shows fields in reversed polarizations and they match very well for all frequencies up to 30 MHz and signal-to-noise ratio has also been improved. Notice that field

characteristics in Figures 4(b) and 4(c) are different because these two sensors are of different calibration factors, which need to be investigated further.

4. Summary

A prototype 0.1 to 30 MHz HFI system was assembled using off-the-shelf components including a magnetic dipole transmitter, and electric and magnetic sensors. The prototype system was tested at sites of different electrical properties demonstrating the proof-of-concept. Encouraged with the initial success, we started to upgrade existing electronic components and antennae to improve the reliability and signal-to-noise ratio of the system. All electronic components will be made as compact as possible. Only optical links will be used to avoid picking up coherent noise from the ambient electric field. The apparent improvement in data quality can be seen from the results of the redesigned electric stub dipole. Similar upgrading is currently under way for the loop transmitter and magnetic field antenna. To acquire data in a frequency-sweeping mode, a network analyzer is being introduced to HFI, and the efficiency of the upgraded system will be greatly improved.

Acknowledgements

This work is supported by the Assistant Secretary for Environmental Restoration and Waste Management, Office of Technology Development of the U.S. Department of Energy under contract No. DE-AC03-76SF00098.

References

Frangos, W., 2001, High Frequency Impedance Measurements for Non-invasive Permittivity Determination, PhD Thesis, University of California, Berkeley.

Lee, K.H., and Becker, A., 2001, High frequency electromagnetic impedance measurements for characterization, monitoring and verification efforts, Interim Report, Project #60328, U.S. DOE.

Song, Y., Kim, H.J., and Lee, K.H., 2002, High-frequency electromagnetic method for subsurface imaging; *Geophysics*, vol. 67, No. 2, pp. 501-510.

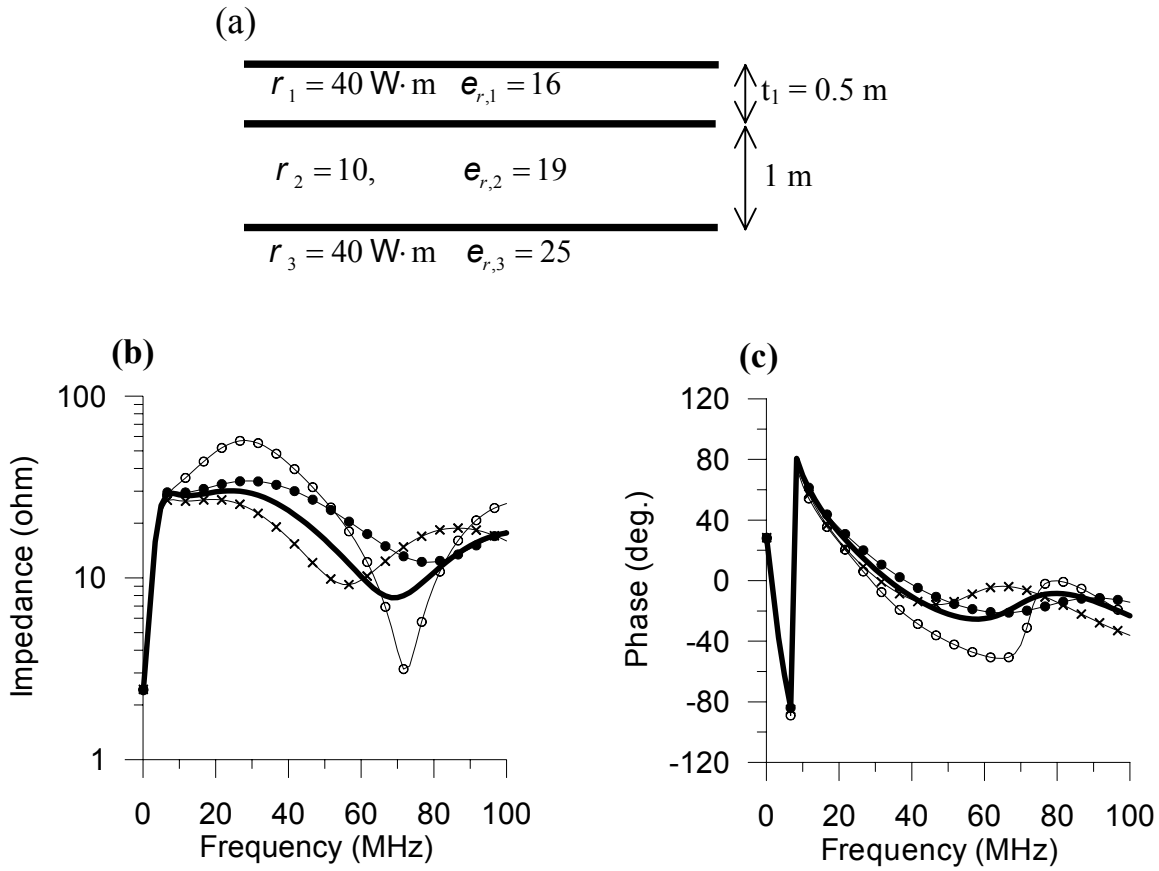

Figure 1. (a) A 3-layered model used to simulate the near-surface electrical structure at a farm site for soil moisture monitoring; (b) and (c) Amplitude and phase of the calculated impedance, respectively. All parameters of the second and bottom layers remain fixed and only the resistivity, r_1, dielectric constant, $e_{r,1}$, and thickness of the first layer, t_1, are changed. For the bold line, $s_1 = 40$ W□m, $e_{r,1} = 16$, t_1=0.5m; for the solid circle, $s_1 = 40$ W□m, $e_{r,1} = 13$, t_1=0.5m; for the open circles, $s_1 = 80$ W□m, $e_{r,1} = 16$, t_1=0.5m; and for the crosses, $s_1 = 40$ W□m, $e_{r,1} = 13$, t_1=0.6 m.

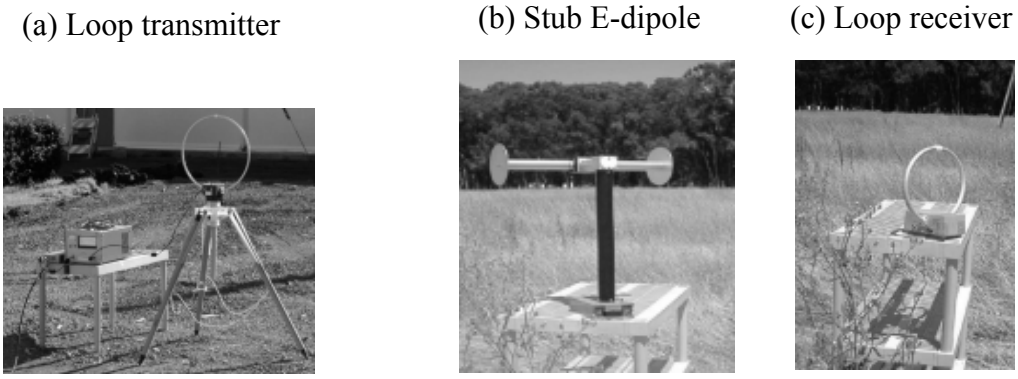

Figure 2. HFI transmitting and receiving antennas: (a) Loop transmitter and related power supply; (b) Electric field sensor with a long supporting beam and a big base plate; (c) Magnetic field sensor.

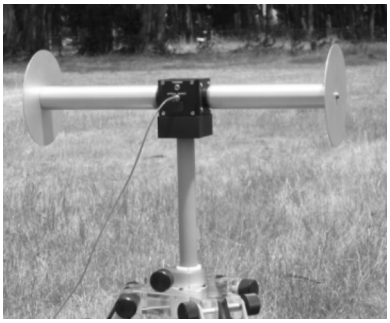

Figure 3. Repackaged electric field sensor.

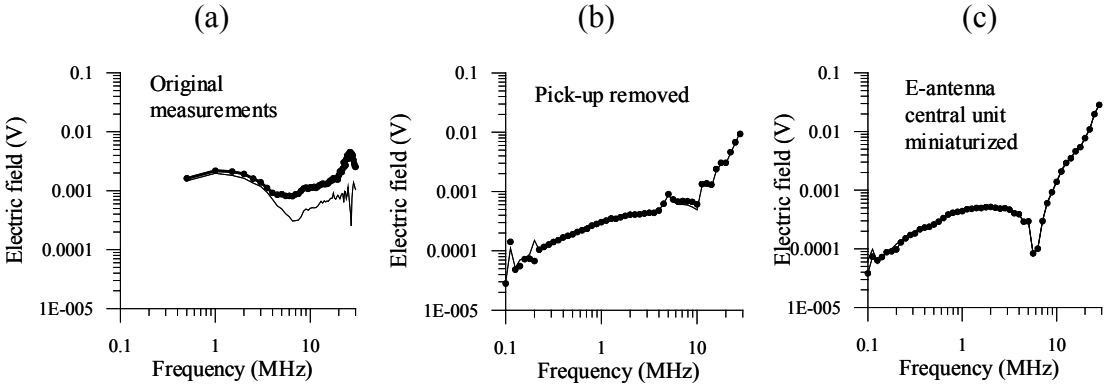

Figure 4. A comparison of electric field measurements between the old and the miniaturized stub antennae: (a) Electric fields measured with the old antenna in normal and reversed polarization; (b) Electric fields with pick-up removed. Pick-up from stub antenna is estimated using measurements from the normal and reversed polarizations; (c) Electric fields in both normal and reversed polarization using the repackaged antenna.